

# Towards New Half-Metallic Systems: Zinc-Blende Compounds of Transition Elements with N, P, As, Sb, S, Se, and Te

Iosif Galanakis and Phivos Mavropoulos\*

*Institut für Festkörperforschung, Forschungszentrum Jülich, D-52425 Jülich, Germany*

(Dated: October 30, 2018)

We report systematic first-principles calculations for ordered zinc-blende compounds of the transition metal elements V, Cr, Mn with the *sp* elements N, P, As, Sb, S, Se, Te, motivated by recent fabrication of zinc-blende CrAs, CrSb, and MnAs. They show ferromagnetic half-metallic behavior for a wide range of lattice constants. We discuss the origin and trends of half-metallicity, present the calculated equilibrium lattice constants, and examine the half-metallic behavior of their transition element terminated (001) surfaces.

PACS numbers: 71.20.Be, 71.20.Lp, 75.50.Cc

## I. INTRODUCTION

The swiftly developing field of spin electronics<sup>1</sup> has provided strong motivation towards the construction of novel magnetic materials. Of particular interest are half-metals, *i.e.* compounds for which only the one spin direction presents a gap at the Fermi level  $E_F$ , while the other has a metallic character. Such behavior is present in various perovskite structures,<sup>2</sup> in Heusler compounds,<sup>3</sup> and in dilute magnetic semiconductors.<sup>4</sup> Lately it has been possible to grow binary CrAs in the zinc-blende (*z-b*) structure epitaxially on GaAs; this compound was found to be half metallic, both by experiment and by relevant calculations.<sup>5</sup> It has also the great advantage of a high Curie temperature  $T_C$ , around 400 K.<sup>6</sup> Similar is the  $T_C$  of ferromagnetic *z-b* CrSb.<sup>7</sup> Moreover, the growth of nanoscale *z-b* MnAs dots on GaAs substrates<sup>8</sup> has been achieved and CrAs/GaAs multilayers have been fabricated.<sup>9</sup> Evidently, the know-how on the construction of these materials, which perhaps can be viewed as the limiting cases of dilute magnetic semiconductors, is increasing, and they will possibly be at the center of interest of spintronics applications soon, since they combine half-metallicity, high Curie temperature, and coherent growth on semiconductor (SC) substrates.

The experimental work on these systems seems to lie ahead of the theoretical analysis. Pioneering calculations concerning the bulk or the surfaces have been reported,<sup>5,10,11,12,13,14,15</sup> but there is still extensive work to be done. One matter to be discussed is the origin of the half-metallicity; another is the question whether half-metallicity is preserved at the surfaces; and a third, in view of the future possible growth of similar compounds based on different SC or transition metals, is the theoretical prediction of the cases where half-metallicity can manifest itself, in order to serve as a helpful guideline to where future experiments can focus. It is the purpose of this paper to address these three points by first-principles calculations.

The outline of the paper has as follows. In Section II we briefly describe our method of calculation. In Section III we address the question of the origin of the half-metallic

behavior and discuss the electronic structure of the *z-b* compounds of transition elements with *sp* atoms; we examine only the ferromagnetic configuration in view of the conclusions of Shirai<sup>11</sup> on VAs, CrAs, and MnAs. In Section IV we present the results of extensive systematic calculations for the *z-b* compounds of the form XY, with X=V, Cr, Mn, and Y=N, P, As, Sb, S, Se, Te, for various lattice constants in a ferromagnetic configuration, and we examine in which cases half-metallicity is present; we also present the calculated equilibrium lattice constants to obtain a feeling for the lattice mismatch if one would grow these compounds on semiconductors. In Section V we focus on the half-metallicity of transition metal terminated (001) surfaces. We conclude with a summary in Section VI.

## II. METHOD OF CALCULATION

To perform the calculations, we have used the Vosko, Wilk and Nusair parameterization<sup>16</sup> for the local density approximation (LDA) of the exchange-correlation potential to solve the Kohn-Sham equations within the full-potential screened Korringa-Kohn-Rostoker (KKR) Green function method,<sup>17</sup> where the correct shape of the Wigner-Seitz cells is accounted for.<sup>18</sup> The scalar relativistic approximation was used, which takes into account the relativistic effects except that of spin-orbit coupling.<sup>19</sup> To calculate the charge density, we integrate along a contour on the complex energy plane, which extends from below the 4*s* states of the *sp* atom up to the Fermi level, using 42 energy points. For the Brillouin zone (BZ) integration we have used a  $\mathbf{k}$ -space grid of  $30 \times 30 \times 30$  in the full BZ (752  $\mathbf{k}$ -points in the irreducible wedge) for the bulk calculations and a  $\mathbf{k}_{\parallel}$ -space grid  $30 \times 30$  (256  $\mathbf{k}_{\parallel}$ -points in the irreducible wedge) in the two-dimensional full BZ for the surface calculations. We have used a cutoff of  $\ell_{\max} = 3$  for the wavefunctions and Green functions. More details on the surface calculations are described in Ref. 14.

The *z-b* structure can be easily seen to fit on a bcc lattice, by occupying only half of the sites with the two kinds of atoms and leaving the other half as voids. Viewed in

this way, the consecutive lattice sites of bcc in the cubic diagonal are occupied by Ga, As, Void1, Void2 (in the case of *e.g.* GaAs). This is useful for the KKR method because all empty space of the quite open z-b structure is taken into account.

We must also say a few words about state-counting with the KKR method. The charge is found by adding the partial contributions of *s*, *p*, *d*, and *f* electrons (if a cutoff of  $\ell_{\max} = 3$  is used). In this way one ignores the contribution to the wavefunction of higher angular momenta, which, although very small, is nonzero. This has a negligible effect for calculations in a metal, where the missing (or extra) charge is regained by a very small readjustment of the Fermi level  $E_F$ . However, if there is a band gap at  $E_F$ , one finds the charge to deviate slightly from the integer value it should have by state-counting. As a consequence for half metals, although the density of states (DOS) and the inspection of the bands show clearly that  $E_F$  lies within the gap for minority spin, and hence the magnetic moment per unit cell must be integer, its calculated value deviates slightly from the exact integer value. In our work, the presence of half metallicity has always been judged by inspection of the density of states and of the energy bands, and not from the value of the magnetic moment. The partial values of the charges and moments, calculated by local orbital summation, are accurate to within 1%.

### III. ELECTRONIC STRUCTURE

In this section we shall examine the electronic structure of the compounds, and discuss the origin of the half metallicity and the value of the total moment. Although for arbitrary  $\mathbf{k}$  the wavefunctions do not belong exclusively to a single irreducible representation such as  $t_{2g}$  or  $e_g$ , it is convenient to retain this terminology for the bands formed by originally  $t_{2g}$  or  $e_g$  orbitals since they are energetically rather separated. Let us focus on a  $3d$  atom. In the z-b structure, the tetrahedral environment allows its  $t_{2g}$  states ( $d_{xy}$ ,  $d_{yz}$ , and  $d_{xz}$ ) to hybridize with the *p* states of the four first neighbors (the *sp* atoms). Note that in the tetrahedral geometry, the *p* orbitals of the four neighboring sites transform as partners of the  $t_{2g}$  irreducible representation when analyzed around the central site.<sup>31</sup> This creates a large bonding-antibonding splitting, with the low-lying bonding states being more of *p* character around the *sp* neighbors (we call these bands “*p*-bands” henceforth), and the antibonding being rather of *d* character around the  $3d$  atom (but see also the discussion below concerning Refs. 10 and 12). The gap formed in between is partly filled by the  $e_g$  states of the  $3d$  atom ( $d_{z^2}$  and  $d_{x^2-y^2}$ ); the position of the gap will be different for majority and minority electrons, due to the exchange splitting.

This symmetry-induced *p-d* hybridization and bonding-antibonding splitting has been found in the past in the case of transition metal doped zinc-blende

semiconductors;<sup>20,21</sup> the splitting has also been referred to as “*p-d* repulsion”, concerning the interaction of the impurity  $t_{2g}$  localized states with the semiconductor anion *p* band. In the limit of full substitution of the semiconductor cation by the transition metal, one arrives to the cases studied here; in particular MnTe has been studied in Ref. 21, and has been found half-metallic if the ferromagnetic phase is assumed.

The situation can be elucidated by examination of the energy bands of CrAs, presented in Fig. 1. The *s* states of As are very low in energy and omitted in the figure. Around  $-3$  eV, the *p*-bands can be seen. The next bands are the ones formed by the Cr  $e_g$  orbitals, around  $-1.5$  eV for majority and  $+1$  eV for minority. They are quite flat, reflecting the fact that their hybridization with the states of As neighbors is weak (or even zero, at  $\mathbf{k} = 0$ , due to symmetry). These bands can accommodate two electrons per spin. Above them, the substantially wider antibonding *p-t<sub>2g</sub>* hybrids appear, starting from  $-1$  eV for majority and from  $+1.5$  eV for minority. Their large bandwidth can be attributed to the strong hybridization and to their high energy position. The bonding-antibonding splitting is also contributing to the fact that they be pushed up beyond the flat  $e_g$  states. As a result, the three families of bands do not intermix, but are rather energetically separate. In the majority-spin direction the bonding-antibonding splitting is smaller, because the transition element  $3d$  states are originally lower in energy, closer to the *p* states of the *sp* atom. In the minority spin direction the states are higher due to the exchange splitting and the gap is around  $E_F$ . Band counting gives an integer total magnetic moment of  $3 \mu_B$ .

To the clear bonding-antibonding gap also the z-b geometry contributes, since it has been previously reported<sup>10,12,13</sup> that in the hexagonal NiAs geometry MnP, MnAs and MnSb show no gap.

Here we must refer to two recent publications on zinc-blende MnAs<sup>10</sup>, and MnP, MnAs, and MnSb,<sup>12</sup> which have identified the *p* and  $t_{2g}$  bands the other way around; *i.e.* they state that the bonding bands are more of *d*-character around Mn and the antibonding more of *p* character around the *sp* atom. This is correct for the majority bands in those compounds where the majority transition-element *d* states are originally lower than the anion *p* states, *e.g.* in the case of the MnAs or CrAs bonding majority bands. For minority-spin the situation is the other way around, so that the bonding bands are more *p*-like centered around the *sp* cation, while the antibonding bands are more *d*-like centered around the transition element. This can be seen by the atom-resolved DOS in Fig. 2. For the group-VI compounds, the *p* states are initially even lower, so that the *p* character of the bonding states increases for both spins.

Next we consider different compounds, to see the trend of increasing transition metal atomic number: VAs, CrAs, MnAs. The corresponding DOS can be seen in Fig. 2, calculated for the InAs lattice parameter in all cases to allow comparison. For VAs,  $E_F$  lies between

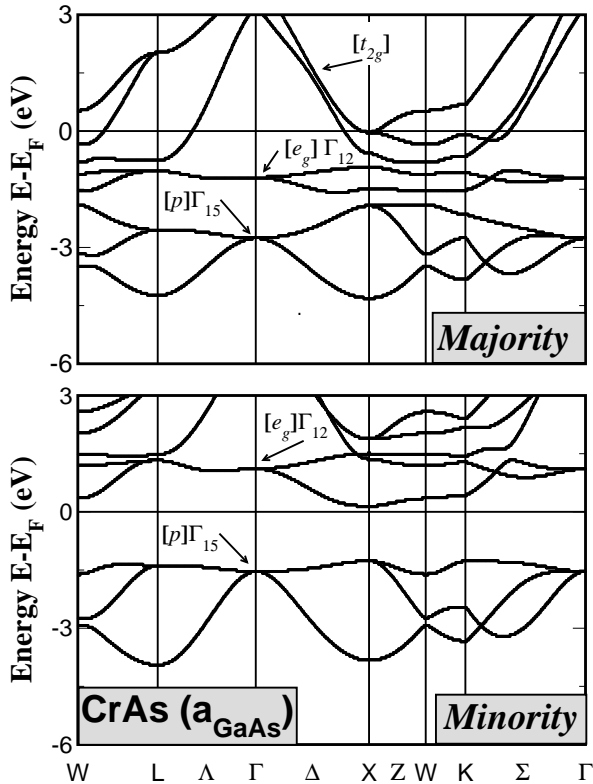


FIG. 1: Energy bands of CrAs calculated at the GaAs lattice constant. With  $p$ ,  $e_g$ , and  $t_{2g}$  we denote the whole bands originating from orbitals of the corresponding character, although this character is well defined only for  $\mathbf{k} = 0$ . The bonding-antibonding splitting between the  $p$  and  $t_{2g}$  bands is evident; the band gap is between the  $p$  and the flat  $e_g$  bands. The system is half-metallic.

the majority  $e_g$  and  $t_{2g}$ . Since they are separated, this results in zero DOS at  $E_F$ , as in the limiting case of a semiconductor with almost zero band gap (shown in more detail in the corresponding inset of Fig. 2). The moment is  $2 \mu_B$ . As the number of valence  $3d$  electrons increases for CrAs, the  $t_{2g}$  bands are pulled down enough to accommodate one electron ( $M = 3 \mu_B$ ), and for MnAs even more, so as to accommodate two electrons, whence  $M = 4 \mu_B$ . At the same time, for the minority spin the band gap does not change in magnitude and continues to embrace  $E_F$ . This can be understood in terms of the exchange splitting  $\Delta E_x$  being proportional to the magnetic moment:  $\Delta E_x \simeq IM$ . When the moment increases by  $1 \mu_B$ ,  $\Delta E_x$  must increase by one time the exchange integral  $I$ , about  $0.8 \text{ eV}$ .<sup>22</sup> Thus the minority bands remain almost at their position.

This behavior is quite stable, unless the energy gained by increasing the exchange splitting in order to achieve one more  $\mu_B$  is overshoot by the Coulomb energy cost; remember that the majority  $t_{2g}$  bands are wide. Then the system compromises by placing  $E_F$  higher, within the minority  $e_g$  conduction band, and half metallicity is

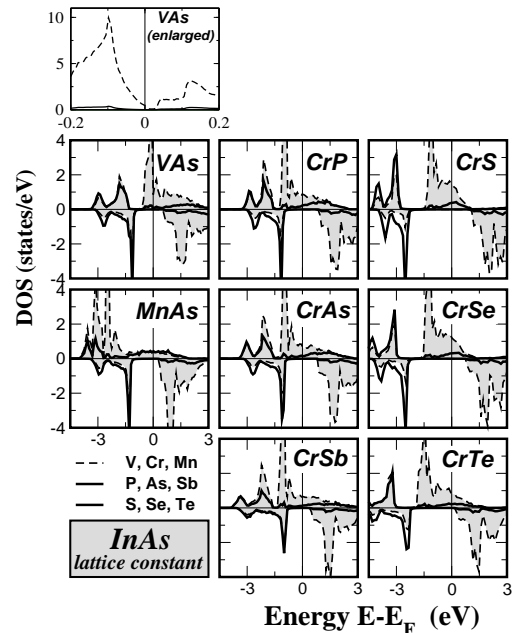


FIG. 2: Atom-resolved DOS for several materials in the  $z$ -b structure using the InAs lattice constant. Negative numbers on the DOS axis represent the minority spin. The dashed lines containing the shadowed area correspond to the DOS within the Wigner-Seitz cell of the transition element, while the full lines to the one of the  $sp$  atom. The small DOS of the vacant sites is omitted. In all cases,  $E_F$  lies within the minority-spin gap, *i.e.* the systems are half-metallic. In the upper left inset, the majority DOS for VAs is shown in more detail around  $E_F$ , to demonstrate the low DOS at  $E_F$ . Spin moments for these compounds are given in Table I.

lost. This can occur for small lattice constants or at the surface, and will be presented in the next sections.

Generally, the bonding  $p$  bands can accommodate 6 electrons (3 per spin), and since they lie low in energy they must be filled up; in addition, there is yet another band lower in energy, consisting of the  $s$  states of the  $sp$  atom, which has space for two electrons (one per spin). Once these 8 bands are filled by 8 of the valence electrons, the remaining electrons will fill part of majority  $d$  states, first the lower-lying  $e_g$  and then the  $t_{2g}$ , creating the magnetic moment. This electron counting gives then an integer total moment of

$$M = (Z_{\text{tot}} - 8) \mu_B, \quad (1)$$

where  $Z_{\text{tot}}$  is the total number of valence electrons in the unit cell.<sup>32</sup> This “rule of 8” is the analogue of the Slater-Pauling behavior for these systems; similar behavior is found in the case of the half-metallic Heusler alloys, as a “rule of 18” or a “rule of 24”.<sup>23,24</sup> Of course these are valid only when half-metallicity is present.

According to the “rule of 8” of Eq. (1), the (integer) moment should increase by  $1 \mu_B$  if one changes only the  $sp$  atom from group V to group VI, since then one more valence electron is available (in this respect there is a

TABLE I: Spin magnetic moment in  $\mu_B$  for the InAs experimental lattice constant. The atomic-resolved moment values refer to the moment included in a Wigner-Seitz cell around each atom. Void1 and Void2 refer to the vacant sites used to describe the zinc-blende structure as described in Section II. The total moment does not appear exactly integer as explained in Section II.

Compound	3dat.	<i>sp</i> -at.	Void1	Void2	Total
CrN	3.887	-1.071	0.027	0.127	2.960
CrP	3.318	-0.448	-0.019	0.085	2.935
CrAs	3.269	-0.382	-0.029	0.080	2.937
CrSb	3.148	-0.249	-0.036	0.084	2.946
VAs	2.054	-0.196	0.006	0.076	1.939
MnAs	4.070	-0.250	0.008	0.106	3.935
CrS	3.858	-0.117	0.050	0.154	3.945
CrSe	3.830	-0.102	0.050	0.162	3.939
CrTe	3.752	-0.057	0.053	0.182	3.930
VSe	2.750	-0.054	0.068	0.173	2.937
MnSe	4.579	0.149	0.061	0.142	4.931

similarity to the dilute magnetic semiconductors<sup>25</sup>). In order to present this, we calculated the electronic structure of the 3*d*-group VI compounds. In Fig. 2 the DOS of CrS, CrSe, and CrTe are shown. We chose to use the InAs lattice constant in this case, so as to compare with the group V compounds at a single lattice constant. Note that the InAs lattice (6.058Å) is very close to the CdSe one (6.052Å). We found a ferromagnetic half-metallic solution for these cases, with a magnetic moment of 4  $\mu_B$  as expected. The physical mechanism involved is the same as in the 3*d*-group V case, and the main difference lies in that *p* states of the group VI elements lie lower in energy, so that the band gap is larger and the hybridization with the neighbor *d* states smaller.

We have also calculated the 3*d*-group VI compounds VS, VSe, VTe, MnS, MnSe, and MnTe. They also show half-metallic behavior for a range of lattice constants, with their magnetic moment given by the “rule of 8”; they will be discussed in the next section. However, we must note that we have only searched for the ferromagnetic solution. A systematic investigation of the energetics of ferromagnetic *vs.* antiferromagnetic solutions lies beyond the scope of this paper. Especially in the case of Mn-group VI compounds, an antiferromagnetic solution could be possibly more stable, since these compounds are isoelectronic with FeAs, which has been found to have an antiferromagnetic ground state at the equilibrium lattice constant in calculations by Shirai;<sup>11</sup> especially MnTe has been calculated to be more stable in the antiferromagnetic phase, in Ref. 21. For the compounds VAs, CrAs, and MnAs, the analysis of Shirai points towards stable ferromagnetic solutions.

In Table I the magnetic moments are presented for several 3*d*-group V and 3*d*-group VI materials for the InAs lattice constants. All these compounds are half-metallic, even MnSe, where the  $t_{2g}$  majority spin band is filled completely to achieve the 5  $\mu_B$ . The total moment,

calculated by summation over KKR local orbitals instead of state counting, does not appear exactly integer as it should, as explained in Section II.

From Table I we see that the *sp* atom has an induced local magnetic moment  $M_{loc}$  opposite to the one of the *d* atom. This is in agreement with previous results on 3*d*-As compounds.<sup>10,11,12</sup> The trend is that for lighter *sp* elements the induced moment absolute value increases ( $M_{loc}$  becomes more negative); naturally, the local moment at the 3*d* atom increases as well, since the total magnetic moment must remain a constant integer. For the group VI elements (higher ionicity) these effects are smaller.

This behavior can be understood in the following way. The minority bonding *p* band is more located within the Wigner-Seitz cell of the *sp* atom, whereas the majority *p* band is more hybridized with the low *d* orbitals and thus more shared with the 3*d* atoms; this results in the opposite magnetic moments of the *sp* atoms. As we change to lighter *sp* elements, the minority *p* wavefunctions become even more localized, while the majority ones are less affected due to their strong hybridisation with the low *d* orbitals (this is evident in the atomic resolution of the DOS of CrSb, CrAs, and CrP in Fig. 2). Thus the absolute value of the local moment on the *sp* atoms — antiparallel to the one of the 3*d* atoms — increases for the lighter elements. In the case of 3*d*-Group VI compounds, these effects are smaller, because the *p* states are deeper in energy, thus less hybridized with the transition element majority *d* states and more alike for the two spin directions.

Another effect of going to lighter *sp* elements is the increase of the band gap, as can be seen in Fig. 2 for CrSb→CrAs→CrP and CrTe→CrSe→CrS. This is consistent with the picture that the local magnetic moment of the 3*d* atom increases, causing a larger exchange splitting  $\Delta E_x$  and pushing up the minority  $e_g$  bands.

#### IV. VARIATION OF LATTICE CONSTANT

The compounds consisting of 3*d* and *sp* elements that have been fabricated<sup>5,7,8</sup> are metastable in the *z*-b structure. For instance, MnAs is grown in the orthorhombic or hexagonal structure,<sup>26</sup> in which it does not present half-metallic behavior,<sup>10,12</sup> although it is still ferromagnetic. The metastable *z*-b structure can be achieved only when the materials are grown on top of a *z*-b semiconductor, such as GaAs.<sup>5,7,8</sup> It can be expected that in the first few monolayers the materials will adopt the lattice constant of the underlying buffer; thus, the question arises whether half-metallicity is present for the lattice parameter of the semiconductor. To peruse this, we have performed calculations of all combinations of the type XY with X=V, Cr, Mn, and Y=N, P, As, Sb, for the lattice constants of the relevant *z*-b III-V semiconductors GaN, InN, GaP, GaAs, InP, InAs, GaSb, and InSb (given in increasing lattice parameter order).

TABLE II: Calculated properties of different materials adopting the zinc-blende structure using the experimental lattice constants  $a$  of several z-b III-V semiconductors. A “+” sign means that a system is half-metallic, a “-” that the Fermi level is above the gap and a “ $\pm$ ” that the Fermi level is only slightly within the conduction band and the spin polarization at  $E_F$  is almost 100%. For each compound, the calculated equilibrium lattice parameter is also given in parentheses. The experimental semiconductor lattice parameters were taken from Refs. 28,29 except for the case of GaN and InN in the zinc-blende structure which were taken from Refs. 28,30.

a(Å)	GaN	InN	GaP	GaAs	InP	InAs	GaSb	InSb
Compound	4.51	4.98	5.45	5.65	5.87	6.06	6.10	6.48
VN (4.21)	-	-	+	+	+	+	+	+
VP (5.27)	-	-	-	+	+	+	+	+
VAs (5.54)	-	-	-	+	+	+	+	+
VSb (5.98)	-	-	-	-	+	+	+	+
CrN (4.08)	-	+	+	+	+	+	+	+
CrP (5.19)	-	-	-	+	+	+	+	+
CrAs (5.52)	-	-	-	+	+	+	+	+
CrSb (5.92)	-	-	-	-	+	+	+	+
MnN (4.06)	-	+	+	+	+	+	+	+
MnP (5.00)	-	-	-	-	+	+	+	+
MnAs (5.36)	-	-	-	-	+	+	+	+
MnSb (5.88)	-	-	-	-	-	-	$\pm$	+

Moreover, we have calculated the equilibrium lattice constant that these compounds would have. In this manner one can obtain a feeling of what systems would perhaps grow on a certain SC substrate, as opposed to unrealistic combinations due to lattice mismatch and stress. Here we must note that within the LDA, the equilibrium lattice constant is known to be underestimated by a few percent<sup>27</sup> (the so-called overbinding); thus the “real” lattice constant of such materials would be as much as 3% larger.

Our results are summarized in Table II. A “+” sign means that the compound is half-metallic for the given lattice constant, while a “-” sign means loss of half-metallicity. A  $\pm$  means that though the system is not half metallic, the spin polarization at  $E_F$  is very close to 100%. Where half-metallicity is preserved, the total magnetic moment is given by Eq. (1). Note that even in the cases where half-metallicity is lost, a  $p$ - $d$  hybridization gap is present (but not at  $E_F$ ). Upon compression, the bandwidth of the valence  $p$ -bands and the  $e_g$  bands increases and the gap between them decreases somewhat — the increase of the bonding-antibonding splitting is not relevant, since it concerns the relative position of the  $p$  and  $t_{2g}$  bands. Most importantly, though,  $E_F$  is shifted towards higher energies by the majority states, so that it can step into the minority  $e_g$  band and destroy half-metallicity. In Table II we see that all materials examined are half-metallic for the large lattice constant of InSb, but lose the half-metallicity for the small one of GaN.

The general trend observed in Table II, apart from the effect of compression, is that the tendency towards half-

TABLE III: Similar to Table II for transition metal compounds with the group VI elements. For each compound, the calculated equilibrium lattice parameter is also given in parentheses. The experimental semiconductor lattice parameters were taken from Ref. 28.

a(Å)	ZnS	ZnSe	CdS	CdSe	ZnTe	CdTe
Compound	5.41	5.67	5.82	6.05	6.10	6.49
VS (5.24)	-	-	+	+	+	+
VSe (5.56)	-	-	-	+	+	+
VTe (6.06)	-	-	-	-	$\pm$	+
CrS (5.04)	-	+	+	+	+	+
CrSe (5.61)	-	$\pm$	+	+	+	+
CrTe (6.07)	-	-	-	+	+	+
MnS (4.90)	-	+	+	+	+	+
MnSe (5.65)	-	-	$\pm$	+	+	+
MnTe (6.10)	-	-	-	-	-	+

metallicity increases for lighter  $sp$  elements. This is consistent with the picture that for lighter group V elements the  $p$  state is energetically lower and also more localized. Both these factors result in reducing the shifting of  $E_F$  by compression; but more importantly, the gap increases for lighter  $sp$  elements as analyzed at the end of Sec. III. Thus half-metallicity holds out longer.

Similar trends are observed in the case of  $3d$ -group VI compounds. The systematics are presented in Table III. The investigated systems are XY with X=V, Cr, and Mn, and Y=S, Se, and Te, for the experimental lattice constants of the II-VI semiconductors ZnS, ZnSe, CdS, CdSe, ZnTe, and CdTe. Again we see the loss of half-metallicity by compression, and a stronger tendency towards half-metallicity for lighter group VI elements; both effects can be attributed to the same reasons as in the  $3d$ -group V case.

However, the calculated equilibrium lattice constants (given in parentheses in Tables II and III) lessen the possible selections. Indeed, the nitrides and sulphides tend to be so much condensed that they would probably not grow epitaxially at a lattice constant favouring half-metallicity; the nitrides are even nonmagnetic at their small equilibrium lattice constant. In fact, only VSb, CrSb and CrTe are half-metallic at their equilibrium lattice constant. On the other hand, if one would allow for a 5% expansion due to the LDA overbinding or tolerable lattice mismatch, one has the possible combinations VAs/GaAs, VSb/InAs, CrAs/GaAs, CrSb/InAs, VTe/CdTe, CrSe/CdS, CrTe/ZnTe.

Other authors have reported results on the equilibrium lattice constant of MnAs, CrAs,<sup>11</sup> VAs,<sup>11</sup> and CrSb.<sup>15</sup> For MnAs, the most frequently studied of these, the reported LDA results are: 5.85 Å (Ref. 11), 5.6-5.7 Å (Ref. 10), 5.45 Å (Ref. 13), and 5.34 Å (Ref. 12). Our calculations give 5.36 Å. We do not know the reason for the discrepancies among the reported values. Changing the  $\ell_{\max}$  cutoff or the number of  $\mathbf{k}$ -points brought only very small changes to our result, while using non-relativistic treatment for the valence electrons resulted in

an increase to 5.41 Å. Results using the generalised gradient approximation (GGA) as an improvement to the LDA have been reported in Refs. 12, 13, and 15, giving slightly larger lattice constants compared with LDA.

## V. (001) SURFACES

In the last part of this paper we examine the possibility of half-metallicity at the surfaces of these compounds. One of the authors (IG) has recently studied the (001) surface of CrAs.<sup>14</sup> The conclusion of that study was that the As terminated surface loses the half-metallicity due to As dangling bonds that form a surface band within the minority spin gap, while the Cr terminated surface retains the half-metallic character and the local magnetic moment increases. This behavior was found for both the GaAs and InAs lattice constants. Here we have extended our calculations to include the VAs and MnAs (001) surfaces, for the InAs lattice constant. The atoms were kept in their ideal bulk-like positions, *i.e.*, we have calculated the unrelaxed and unreconstructed surface; we must note that large relaxations or reconstruction could alter the half-metallic character of the surface. Since for the As terminated surfaces the surface states originating from dangling bonds cannot be avoided, we will discuss the termination with the 3d atom. Although at the surface the  $t_{2g}$  and  $e_g$  representations are no longer relevant (the former splits in two, one containing  $d_{xz}+d_{yz}$  and one  $d_{xy}$ , and the latter also in two, one containing  $d_{x^2-y^2}$  and one  $d_{z^2}$ ), we ask for understanding that we continue to use the same terminology in order to make the connection to the bulk states.

The DOS for the VAs and MnAs (001) surfaces are shown in Fig. 3, for both the atom at the surface layer (V or Mn) and at the subsurface layer (As). For comparison, the corresponding DOS in the bulk are also presented. Evidently the V terminated VAs (001) surface remains half-metallic. However, there is an important difference in the DOS as compared to the bulk case, especially at the surface (V) layer. For the majority spin, the peak at around  $-2$  eV is strongly reduced, and the same happens for the minority spin at around  $-1$  eV. This can be explained by the fact that the surface V atom has a reduced coordination number of only two As neighbors. Then two less As  $p$  orbitals penetrate the V cell, reducing the local weight of the bonding states. At the same time, the majority peak just under the Fermi level is enhanced, gaining the weight which has been lost by the bonding states from both spin directions. Note in the DOS of the V surface atom that there is no more the clear minimum at  $E_F$  for the majority states, which was distinguishing  $e_g$  from  $t_{2g}$  in the bulk, as the reduced bonding-antibonding splitting allows the latter states to come lower in energy.

In terms of electron counting, the V atoms in the bulk give away 3 of the 5 valence electrons to the  $p$  band and retain the remaining two to build up the magnetic mo-

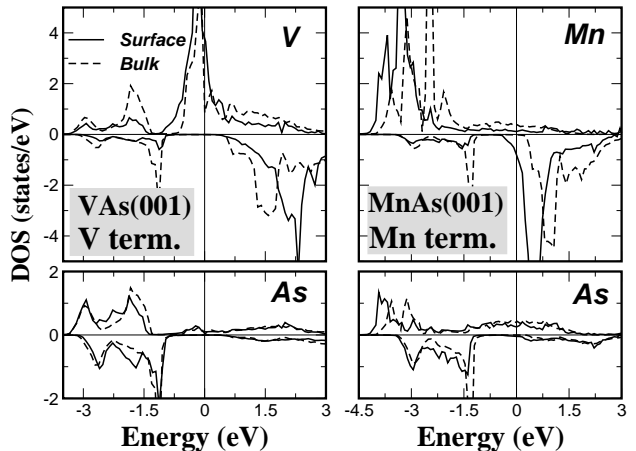


FIG. 3: Left panel: Spin- and atom-resolved DOS of the V-terminated (001) surface for the V atom at the surface layer and the As atom at the subsurface layer for the InAs lattice constant (left panel). The surface DOS (full lines) and the bulk DOS (dashed lines) are shown. The As  $s$  states are located at around 10 eV below the Fermi level and are not shown in the figures. The energy zero refers to  $E_F$ ; negative numbers on the DOS axis represent the minority spin. Right panel: Same for the Mn-terminated MnAs (001) surface.

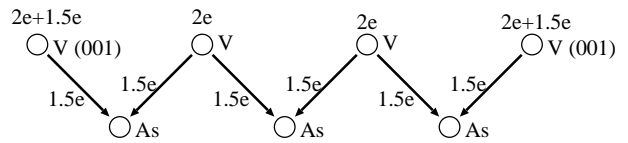


FIG. 4: Schematic interpretation of the origin of the excess moment of  $1.5 \mu_B$  at the VAs surface. The arrows represent the donation of V electrons to the valence band generated mainly by the low-lying As  $p$  orbitals. At the V-terminated (001) surface, half the neighbors of the V atom are missing, so an excess of 1.5 electrons remains. They occupy the majority-spin states, giving an extra  $1.5 \mu_B$ . The situation is similar in all 3d-group V compounds; for the 3d-group VI compounds the  $p$  band welcomes in total 2 instead of 3 electrons from each 3d atom, thus the excess moment is 1 instead of  $1.5 \mu_B$ .

ment. On the other hand, due to the reduced coordination at the surface, only 1.5 electron per V atom is given away, thus 3.5 remain to fill up majority states and build up the magnetic moment; due to the gap, the minority states cannot take over any of these extra electrons, unless  $E_F$  moves higher into the  $e_g$ -like band (this is the case for Mn to which we shall turn shortly). The situation is given schematically in Fig. 4.

The gain in magnetic moment at the surface is accompanied by an increase of the exchange splitting, pushing the antibonding and  $e_g$ -like minority peaks higher in energy (from 1.5 eV to 2 eV); otherwise the gap could have decreased due to reduced hybridisation.

The increased magnetic moment must reach  $3.5 \mu_B$  in the vicinity of the surface; we find that  $3.07 \mu_B$  are lo-

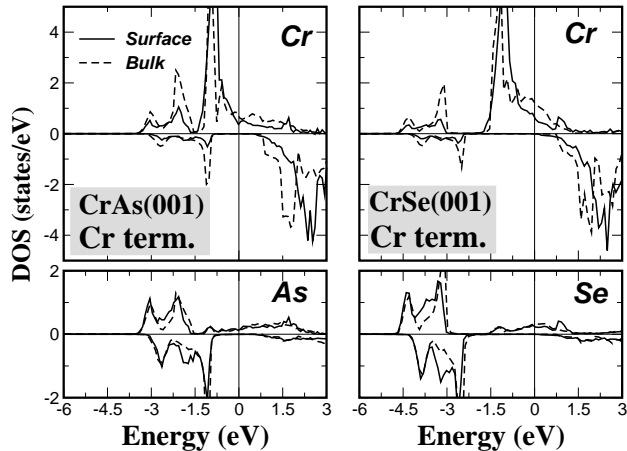


FIG. 5: Spin- and atom-resolved DOS of the Cr-terminated CrAs and CrSe (001) surfaces for the Cr atom at the surface layer and the As and Se atoms at the subsurface layer for the InAs lattice constant. The As and Se  $s$  states are located at around 10 eV below the Fermi level and are not shown in the figures. The surface DOS are compared to the bulk calculations (dashed lines). The energy zero refers to  $E_F$ ; negative numbers on the DOS axis represent the minority spin.

cated on the surface layer, about  $0.35 \mu_B$  in the vacuum, and the rest adds up to the moment of the subsurface layer. We see that the integer value of the magnetic moment, which is mandatory in bulk half-metallicity, ceases to be a prerequisite in the vicinity of the surface.

The situation described here is completely analogous to the one of the CrAs (001) surface.<sup>14</sup> There, the magnetic moment of the surface layer was reported to reach  $4 \mu_B$ ; if the magnetic moment of the vacuum and the subsurface layer is added, one finds a total moment of  $4.5 \mu_B$  in the vicinity of the surface, *i.e.*  $1.5 \mu_B$  more than in the bulk.

However, things are different for MnAs (001) (with Mn termination). The corresponding DOS of the surface Mn atom and of the subsurface As atom is shown in Fig. 3 (right panel). Manifestly, half-metallicity has been lost. The difference to the VAs and CrAs cases lies in the high magnetic moment of  $4 \mu_B$  that MnAs already shows in the bulk. If its moment were to increase by the same mechanism, the surface (plus vacuum and subsurface layers) would have to accommodate 5.5 majority spin electrons. This is energetically unfavorable, since the extra half electron cannot be accommodated by the  $t_{2g}$  band, so that higher-lying bands would have to be populated. Instead, as the majority states are lowered, the slow gain in magnetic moment is not enough to increase the exchange splitting substantially, and the minority  $d$  states also reach  $E_F$ . As a net result, majority and minority DOS peaks are substantially lower in energy, half-metallicity is lost, and a total magnetic moment of  $4.59 \mu_B$  is present within the first surface layer.

We have also made calculations for the X terminated XSe(001) surfaces, where X=V, Cr, and Mn, using the InAs lattice constant. The V and Cr ones are half-

metallic while the Mn surface is not half-metallic. The arguments in the above paragraphs still hold, but now each V, Mn or Cr atom loses Se (group VI) neighbors instead of As (group V) and thus the electron counting changes. In the bulk each X atom gives away only 2 electrons to the  $p$  band and not 3 as in the XAs compounds. Losing two neighbors means that the surface X atom gives away now only 1 electron, so we should have now 4 electrons for V or 5 electrons for Cr to build up the spin moment, *i.e.* we should have  $1 \mu_B$  more than in the bulk. Indeed we find the total spin moment to increase to  $4 \mu_B$  for VSe(001) and  $5 \mu_B$  for CrSe(001). The MnSe compound cannot be half-metallic as this would mean a total spin moment of  $6 \mu_B$  at the surface which is energetically unfavourable for reasons similar to the MnAs surface.

A comparison of the CrAs(001) with the CrSe(001) surface DOS, both Cr terminated and at the InAs lattice constant, is shown in Fig. 5, where the bulk DOS is also presented. We see that the differences in the bulk of the two materials (larger gap, more weight in the majority states under  $E_F$  to account for one more electron) remain their major differences also in the surfaces.

## VI. SUMMARY AND CONCLUSION

We have studied zinc-blende compounds of the transition metal elements V, Cr, Mn with the group V  $sp$  elements N, P, As, Sb and the group VI S, Se, Te, in the ferromagnetic configuration. They all show a tendency towards half-metallic behavior, *i.e.* 100% spin polarization at  $E_F$ . This can be traced back to the bonding-antibonding splitting due to hybridization between the transition element  $d$  ( $t_{2g}$ ) states and the  $sp$  element  $p$  states, conspiring with the large exchange splitting which pushes up the minority  $d$  states. The total moment per unit cell, if the system is half-metallic, is integer and given by the “rule of 8”. Also, the  $sp$  atoms are found to have an antiparallel local moment with respect to the  $3d$  atoms; the absolute value of the local moments increases for lighter or less ionized  $sp$  elements. This is traced back to the degree of localization of the  $p$  wavefunctions around the  $sp$  atoms.

We have discussed the trends with varying lattice constant, in view of the possibility to grow these materials epitaxially on various semiconductors, and calculated the LDA equilibrium lattice constants to obtain a feeling of the lattice mismatch with the possible SC substrates. Compression eventually kills half-metallicity, since  $E_F$  finally wanders above the minority gap. Although for compounds involving lighter  $sp$  elements half-metallicity seems more robust, there equilibrium lattice constants are too small. Thus, the best candidates for half-metallicity from this aspect are VAs, VSb, CrAs, CrSb, VTe, CrAs, and CrTe.

Finally, we have examined the behavior of the transition element terminated (001) surfaces. In most cases

half metallicity is maintained, and the magnetic moment increases because of the missing neighbours where charge would be transferred. Exceptions are the cases where the surface magnetic moment should exceed  $5 \mu_B$ , for which half metallicity is lost.

In view of recent experimental success to grow such compounds, and of their relevance to the field of spintronics, we believe that our work will not only add to the understanding of these systems, but will also contribute to the future realization of spintronics devices.

### Acknowledgments

Financial support from the RT Network of *Computational Magnetoelectronics* (contract RTN1-1999-00145)

- 
- \* Electronic address: Ph.Mavropoulos@fz-juelich.de
- <sup>1</sup> G. A. Prinz, *Science* **282**, 1660 (1998).
  - <sup>2</sup> R. J. Soulen Jr., J. M. Byers, M. S. Osofsky, B. Nadgorny, T. Ambrose, S. F. Cheng, P. R. Broussard, C. T. Tanaka, J. Nowak, J. S. Moodera, A. Barry, and J. M. D. Coey, *Science* **282**, 85 (1998).
  - <sup>3</sup> R. A. de Groot, F. M. Mueller, P. G. van Engen, and K. H. J. Buschow, *Phys. Rev. Lett.* **50**, 2024 (1983).
  - <sup>4</sup> F. Matsukura, H. Ohno, A. Shen, and Y. Sugawara, *Phys. Rev. B* **57**, R2037 (1998).
  - <sup>5</sup> H. Akinaga, T. Manago, and M. Shirai, *Jpn. J. Appl. Phys.* **39**, L1118 (2000).
  - <sup>6</sup> M. Mizuguchi, H. Akinaga, T. Manago, K. Ono, M. Oshima, and M. Shirai, *J. Magn. Magn. Mater.* **239**, 269 (2002).
  - <sup>7</sup> J. H. Zhao, F. Matsukura, K. Takamura, E. Abe, D. Chiba, and H. Ohno, *Appl. Phys. Lett.* **79**, 2776 (2001).
  - <sup>8</sup> K. Ono, J. Okabayashi, M. Mizuguchi, M. Oshima, A. Fujimori, and H. Akinaga, *J. Appl. Phys.* **91**, 8088 (2002).
  - <sup>9</sup> M. Mizuguchi, H. Akinaga, T. Manago, K. Ono, M. Oshima, M. Shirai, M. Yuri, H. J. Lin, H. H. Hsieh, and C. T. Chen, *J. Appl. Phys.* **91**, 7917 (2002).
  - <sup>10</sup> S. Sanvito and N. A. Hill, *Phys. Rev. B* **62**, 15553 (2000).
  - <sup>11</sup> M. Shirai, *Physica E* **10**, 143 (2001).
  - <sup>12</sup> A. Continenza, S. Picozzi, W. T. Geng, and A. J. Freeman, *Phys. Rev. B* **64**, 085204 (2001).
  - <sup>13</sup> Y.-J. Zhao, W. T. Geng, A. J. Freeman, and B. Delley, *Phys. Rev. B* **65**, 113202 (2002).
  - <sup>14</sup> I. Galanakis, *Phys. Rev. B* **66**, 012406 (2002).
  - <sup>15</sup> B.-G. Liu (unpublished); preprint in arXiv:cond-mat/0206485
  - <sup>16</sup> S. H. Vosko, L. Wilk, and N. Nusair, *Can. J. Phys.* **58**, 1200 (1980).
  - <sup>17</sup> N. Papanikolaou, R. Zeller, P. H. Dederichs, *J. Phys.: Condens. Matter* **14**, 2799 (2002).
  - <sup>18</sup> N. Stefanou, H. Akai, and R. Zeller, *Comp. Phys. Commun.* **60**, 231 (1990); N. Stefanou and R. Zeller, *J. Phys.: Condens. Matter* **3**, 7599 (1991).
  - <sup>19</sup> S. Blügel, H. Akai, R. Zeller, and P. H. Dederichs, *Phys. Rev. B* **35**, 3271 (1987).
  - <sup>20</sup> A. Zunger and U. Lindefelt, *Phys. Rev. B* **27**, 1191 (1983); V. A. Singh and A. Zunger, *Phys. Rev. B* **31**, 3729 (1985); S.-H. Wei and A. Zunger, *Phys. Rev. B* **37**, 8958 (1988).
  - <sup>21</sup> S.-H. Wei and A. Zunger, *Phys. Rev. B* **35**, 2340 (1987).
  - <sup>22</sup> O. Gunnarsson, *J. Phys. F* **6**, 587 (1976); J. F. Janak, *Phys. Rev. B* **16**, 255 (1977). In the latter reference the exchange integral is by definition half the one used here.
  - <sup>23</sup> I. Galanakis, P. H. Dederichs, and N. Papanikolaou, *Phys. Rev. B* **66**, 134428 (2002).
  - <sup>24</sup> I. Galanakis, N. Papanikolaou, and P. H. Dederichs, *Phys. Rev. B to be published*; Preprint in arXiv:cond-mat/0205129 (2002).
  - <sup>25</sup> K. Sato (private communication).
  - <sup>26</sup> V. M. Kaganer, B. Jenichen, F. Schippan, W. Braun, L. Däweritz, and K. H. Ploog, *Phys. Rev. Lett.* **85**, 341 (2000).
  - <sup>27</sup> M. Asato, A. Settels, T. Hoshino, T. Asada, S. Blügel, R. Zeller, and P. H. Dederichs, *Phys. Rev. B* **60**, 5202 (1999).
  - <sup>28</sup> Landolt-Börnstein, New Series, Group III, Vol. 17, Pt.a edited by O. Madelung, Springer-Verlag, Berlin (1982).
  - <sup>29</sup> Landolt-Börnstein, New Series, Group III, Vol. 22, Pt.a edited by O. Madelung, Springer-Verlag, Berlin (1986).
  - <sup>30</sup> Landolt-Börnstein, New Series, Group III, Vol. 41, Pt.A1a edited by U Rössler, Springer-Verlag, Berlin (2001).
  - <sup>31</sup> Again, this is strict only for  $\mathbf{k} = 0$
  - <sup>32</sup> The cumbersome electron counting can be avoided by just observing that  $M = N_{\text{maj}} - N_{\text{min}} = N_{\text{maj}} + N_{\text{min}} - 2 \times N_{\text{min}} = Z_{\text{tot}} - 2 \times N_{\text{min}}$ , where  $N_{\text{maj}}$  and  $N_{\text{min}}$  are respectively the numbers of majority and minority valence electrons.